Manuscript

Two effective methods for impedance estimation in distance relays based on the DC offset removal

Alejandro Zamora-Mendez, Julian Sotelo-Castañón, Mario R. Arrieta Paternina, Paola Buendia, Cristian Torres, Carlos Toledo-Santos, Victor Velasco, Francisco Zelaya-A., and Gabriel E. Mejia-Ruiz

***Abstract*—This paper introduces the eigensystem realization (ER)-based identification algorithm and the Z-domain method (ZDM) to improve the impedance estimation of transmission lines under fault conditions, which is achieved by removing the exponential decaying DC offset from current signals in distance relays. Both methods effectively work employing a one-cycle rectangular window; specifically, the Z-domain method works in less than a fifth of one-cycle window, ensuring timely, accurate, and prompt estimates. To confirm the effectiveness and performance of the proposed algorithms, they are evaluated under steady-state and dynamic conditions by using time-domain simulations performed in PSCAD© and DIgSILENT©PowerFactory. They also are compared with the well-known discrete Fourier transform (DFT). The attained results indicate that both the ER-based and Z-domain methods can become a powerful tool to reduce the adverse influence of exponentially decaying DC offsets in distance relays.**

***Keywords*—Eigensystem realization algorithm, Z-domain, phasor estimation, distance relay, impedance estimation, DC offset.**

I. Introduction

ACCURATE voltage and current phasors are frequently used to furnish protection functions in digital relays. Becoming their accuracy and time-response the main characteristics to assess any algorithm for impedance estimation in digital distance relays. In this context, many digital algorithms have been proposed in the last two decades [1]–[11], being the discrete Fourier transform (DFT)-based algorithms the most employed to estimate such phasors [12]. One of their advantage is its straightforward implementation and low computational complexity. Nevertheless, when exponential decaying DC offsets are present in current channels under fault conditions, the DFT exhibits an error yielding a tendency of overreach or underreach phenomena in distance relays [13], [14]. This fact represents a challenging problem that must be taken into consideration to estimate phasors at the fundamental frequency.

To tackle the phasor estimation problem derived from the presence of exponential decaying DC components, different methods have been introduced to accomplish the phasor estimation by mitigating the exponential decaying DC effects. This is achieved by post-processing the data or extending the analysis data window [13], [15]. However, the accuracy of these methods does not only depend on the correct estimation at the fundamental frequency, but it also relies on the suppression of other frequency components; meanwhile the time-response is highly depending on the length of the analysis window [16].

Conventionally, methods such as the mimic circuit are employed to mitigate the DC component effect [13], [17]. The mimic filter may completely remove the decaying DC offset only when exist a match between the actual and presumed time constants of the DC offset [13]. It uses the X/R ratio of a burden circuit which should be equal to the X/R system ratio. However, the X/R ratio varies with the network switching and fault arc resistance. The best performance of the mimic filter arises when its time constant becomes equal to the current time constant.

Other methods report the modified Fourier algorithms such as the DFT-based full and half cycle to convey the phasor correction concerning the error at the DFT output caused by the exponential decaying DC component [6]–[8], whose main difference consists of the ability of eliminating harmonics. Another Fourier-based method, named IDFT, is also able to mitigate the decaying DC component presented [18].

Other proposals use the least squares (LS) algorithm, or the combination of the Fourier-based method with the wavelet transform (WT), the empirical mode decomposition (EMD), the cosine filter, among others [2]–[8], [19]–[21]. For instance, the LS algorithm estimates phasors by removing the DC offset [4]. This approach models the first two terms of the Taylor series expansion over a wide range of time constants from 0.1 to 0.5 cycles. A recursive LS aided by a morphological filter is proposed to provide phasors for transmission line protection, being tested in distance relays attaining better results than the DFT [22]. A DFT-based method combined with WT is proposed in [2] to estimate the decaying DC characteristic of the current signal and compensate the effect of the decaying DC on the current phasor estimation. Furthermore, this problem has been solved by the EMD technique [3]. All these strategies exhibit higher computational complexity than those driven by the DFT, which ostensibly increments the phasor estimation time.

In [6], the decaying DC parameters are estimated using three successive full cycle DFT outputs. Modified algorithms are proposed in [7], which are based on partial sums of one-cycle. In [8], the decaying DC component effect on phasor estimation is suppressed using the difference between the outputs of the full cycle discrete Fourier transform for the odd-sample set and even-sample set. The cosine filter in [5] has been proposed as alternative to suppress the decaying DC component from phasors. It uses the orthogonality between the present and the quarter-cycle earlier outputs of the full cycle cosine filter. However, it delays the response time by a quarter of a cycle.

Alternatively, artificial neural networks-based algorithms are also intended to be incorporated in distance relays [23]–[25]. Recently, with the increase of data science, these have been brought back introducing new approaches to estimate phasors and line impedance for protection functions [9], [10]. Despite these techniques exhibit suitable performances, they require previous and continue training stages that may convey to provide

A. Zamora is with the Electrical Engineering Faculty, at the Michoacan State University, Morelia, Michoacan 58030, Mexico, (e-mail: azamoram@umich.mx).

J. Sotelo is with the Mechanical and Electrical Engineering Faculty, at the University of Guadalajara, Guadalajara, JAL 44430, Mexico, (e-mail: julian.sotelo@academicos.udg.mx).

M. R. A. Paternina, P. Buendia, C. Torres, V. Velasco, and G. Mejia-Ruiz are with the National Autonomous University of Mexico (UNAM), Mexico City 04510, Mexico, (e-mails: mra.paternina@fi-b.unam.mx, paola_290395 [criis_21][victor_vel][gabriel.mejia.ruiz]@comunidad.unam.mx).

C. Toledo is with the Industrial University of Santander (UIS), Bucaramanga 680001, Colombia, (e-mail: carlos.toledo@correo.uis.edu.co).

F. Zelaya is with the University of Tennessee, Knoxville, USA, (e-mail:fzelayaa@vols.utk.edu).

Authors acknowledge financial support from DGAPA, PAPIIT-2021 through the project TA101421. Also, they gratefully thank to the CEMIE-Redes, strategic project PE-A-04.

inaccurate results at the beginning or during the estimation process, thus are completely dependent on the training stage.

To effectively and precisely address the above mentioned problems in distance relays, this investigation introduces the ER-based and Z-domain methods for impedance estimation in distance relays. They are powered with the ability of removing the exponential decaying DC offset from faulted signals, improving the impedance estimation for digital relaying functions. Their performances are compared with the DFT. The attained results indicate that both methods are less sensitive to the exponential decaying DC, which may appear following any disturbance in power systems. Likewise, they provide faster time response than the DFT under transitory behaviors. Their effectiveness is due to their ability to render phasor estimates in a one-cycle rectangular window with enough precision. Furthermore, the Z-domain method (ZDM) can provide estimates in a short window of a few samples depending on the number of components. Additionally, the proposals enable to improve the frequency computation and its tracking since the ER-based and Z-domain estimators are frequency adaptive methods that allow better estimates.

Specifically, the primary contributions of the paper are, as follows:

1) Both proposed methods are equipped with a non-stationary signal model which make them to be considered as dynamic phasor estimators, since they can provide synchrophasor estimates such as amplitude, phase angle, and frequency at one-cycle or less, with the advantage of being adaptable to the operating conditions.
2) The proposed filters improve the relay's steady-state and transient responses with respect to the well-known DFT, thanks to the removal of the DC component and preventing the oscillatory behavior in the impedance estimation.
3) The proposals improve the operating time under fault and oscillatory conditions, providing reliable trips because they reliably and rapidly remove the exponential decaying component in the current signals.

The remaining sections of the paper are organized as follows. Section II details the mathematical fundamentals for the ER-based and Z-domain methods. Then, the test cases under study are described in Section III. The effectiveness and performance of the proposed method is extensively assessed by frequency response and time-domain simulations in Section IV. Finally, concluding remarks are indicated in Section V.

II. Mathematical Foundations of the Proposed Methods

In this section, the ER-based system identification and ZDM methods are described aiming to estimate voltage and current phasors with the capability of performing a DC offset removal. Such phasor estimates sustain a digital relaying strategy for distance relays, since the phasor information is vital in line impedance estimation under fault conditions.

A. Eigensystem Realization Model

This section is devoted to describe the ER-based system identification technique to precisely estimate the instantaneous current signals' DC offset. To carry out the eigensystem realization, a linear model identification problem is stated by establishing the input and output relationship. Where the input sequence is assumed as known, whereas the output may be either measured or recorded to the influence of the input sequence, which can be assumed as a noiseless series in discrete time. Both sequences are correlated via the Markov's parameters ($\mathbf{A}$, $\mathbf{B}$, $\mathbf{C}$, and $\mathbf{D}$) as [26]:

$$\begin{aligned} y(0) &= \mathbf{D}u(0) \\ y(1) &= \mathbf{CB}u(0)+\mathbf{D}u(1) \\ y(2) &= \mathbf{CAB}u(0)+\mathbf{CB}u(1)+\mathbf{D}u(2) \\ &\vdots \\ y(N-1) &= \mathbf{CA}^{N-1}\mathbf{B}u(0)+\cdots+\mathbf{CB}u(N-1)+\mathbf{D}u(N-1) \end{aligned} \tag{1}$$

This can also be synthesized as [26]:

$$\mathbf{y}(k)=\mathbf{CA}^{k-1}\mathbf{B} \tag{2}$$

Thereby, the following linear time-invariant state-space model in discrete-time can be shaped [26]

$$\begin{aligned} \mathbf{x}(k+1) &= \mathbf{Ax}(k)+\mathbf{Bu}(k) \\ \mathbf{y}(k) &= \mathbf{Cx}(k)+\mathbf{Du}(k) \end{aligned} \tag{3}$$

Where the state vector in discrete-time is represented by

$$\mathbf{x}(k)=\mathbf{A}^{k-1}\mathbf{B} \tag{4}$$

In terms of a Hankel representation for the k-th output sample recorded, this becomes [26]–[28]:

$$\mathbf{H}(k)=\begin{bmatrix} y(k) & y(k+1) & \cdots & y(k+N) \\ y(k+1) & y(k+2) & \cdots & y(k+N+1) \\ \vdots & \vdots & \ddots & \vdots \\ y(k+N) & y(k+N+1) & \cdots & y(k+2N) \end{bmatrix} \tag{5}$$

Then, the relationship between the k-th output sample recorded and the Hankel representation is given by [26]–[28]

$$H(k)=\begin{bmatrix} \mathbf{CA}^{k-1}\mathbf{B} & \mathbf{CA}^{k}\mathbf{B} & \cdots & \mathbf{CA}^{k-1+n}\mathbf{B} \\ \mathbf{CA}^{k}\mathbf{B} & \mathbf{CA}^{k+1}\mathbf{B} & \cdots & \mathbf{CA}^{k+n}\mathbf{B} \\ \vdots & \vdots & \ddots & \vdots \\ \mathbf{CA}^{k-1+n}\mathbf{B} & \mathbf{CA}^{k+n}\mathbf{B} & \cdots & \mathbf{CA}^{k-1+2n}\mathbf{B} \end{bmatrix} \tag{6}$$

Which it can be generalized by [27], [28]

$$\mathbf{H}(k)=\underbrace{\begin{bmatrix} \mathbf{C} \\ \mathbf{CA} \\ \vdots \\ \mathbf{CA}^{n} \end{bmatrix}}_{\boldsymbol{\xi}} \mathbf{A}^{k-1}[\mathbf{B} \quad \mathbf{AB} \quad \cdots \quad \mathbf{A}^{n}\mathbf{B}] \tag{7}$$

where $\boldsymbol{\xi}$ in (7) indicates the reachability and the term $\mathbf{A}^{k-1}\mathbf{B}$ symbolizes the controllability.

If only the output samples $k=1$ and $k=2$ are taken into consideration in (7), then we have

$$\begin{aligned} H(1) &= \boldsymbol{\xi}B \\ H(2) &= \boldsymbol{\xi}AB \end{aligned} \tag{8}$$

Finally, it is possible to estimate the Markov parameters from (8) by means of the singular value decomposition (SVD) applied to $H(1)\in\Re^{N\times N}$ and its truncation up to the r-th singular values (with $r<N$), implying a full rank for the system [29]. The SVD results in the form of $H(1)=PSQ^T$, where P and Q are matrices that contain the left and right singular vectors, respectively, whereas S is a diagonal matrix of singular eigenvalues (≥ 0). Thus, the order of the system will be the number of nonzero singular values. Then, $H(1)$ can be notated as $H(1)=PS^{1/2}S^{1/2}Q^T$, which derives that $\boldsymbol{\xi}=PS^{1/2}$ and $B=S^{1/2}Q^T$ in (8), gaining the state-space matrices in discrete-time as [26]

$$\begin{aligned} \mathbf{A} &= S^{-1/2}P^TH(2)QS^{-1/2} \\ \mathbf{B} &= S^{1/2}Q^T \\ \mathbf{C} &= PS^{1/2} \\ \mathbf{D} &= y(0) \end{aligned} \tag{9}$$

Once the identified linear model for one output channel is available, a second stage is advocated to deal with the phasor estimation process [30]. Whose signal model is described by the following sum of complex exponential functions:

$$y(t)=\sum_{k=1}^{K} Re\{a_k e^{j\varphi_k} e^{(\sigma_k+j2\pi f_k)t}\} \tag{10}$$

where K is the number of complex exponential components, $p_k=a_k e^{j\varphi_k}$ represents the k-th residue, and $\zeta_k=\sigma_k+j\omega_k$ corresponds to the signal eigenvalues, with $\omega_k=2\pi f_k$. All of them are computed from the state matrix $\mathbf{A}$ in (9) as $\lambda(\mathbf{A})=\{\zeta_1,\zeta_2,...,\zeta_n\}$. With signal eigenvalues, the residues can be found by [30]

$$\underbrace{\begin{bmatrix} \zeta_1 & \zeta_2 & \cdots & \zeta_n \\ \zeta_1^2 & \zeta_2^2 & \cdots & \zeta_n^2 \\ \vdots & \vdots & \ddots & \vdots \\ \zeta_1^N & \zeta_2^N & \cdots & \zeta_n^N \end{bmatrix}}_{Z} \begin{bmatrix} p_1 \\ p_2 \\ \vdots \\ p_n \end{bmatrix} = \begin{bmatrix} y(1) \\ y(2) \\ \vdots \\ y(N) \end{bmatrix} \tag{11}$$

where $y(k)$ are the output measurements and the matrix $\mathbf{Z}$ is a Vandermonde matrix [30].

$$\hat{p}=(Z^H Z)^{-1} Z^H y \tag{12}$$

where H is the Hermitian transpose operator, y is the measured signal, and $\hat{p} = [p_1 \quad \bar{p}_1]$ contains the residues. Then, the relationships for the phasor estimates (amplitude $\hat{a}$, phase $\hat{\varphi}$, and frequency $\hat{f}$)are established by [30],

$$\begin{aligned} \hat{a} &= 2|p_1| \\ \hat{\varphi} &= p_1 \\ \hat{f} &= \mathrm{Im}\left(\frac{\ln\zeta}{2\pi\Delta t}\right) \end{aligned} \tag{13}$$

To estimate the DC offset of instantaneous current signals, a value of $K = 3$ is chosen to obtain a pair of complex conjugates corresponding to the fundamental frequency and the DC component.

B. Z-domain Method

This paper also proposes a method based on Z-transform known as the Z-domain method (ZDM) [31], [32]. The ZDM characterizes functions that compose a multi-component signal aiming to estimate their amplitud, frequency, phase angle, damping constant, and direct current component. Thus, the signal model for the phasor estimation and DC offset removal can be written as follows [31]:

$$s(t)=A\cos(2\pi f_1 t+\varphi)+\xi^t \tag{14}$$

where A stands for the amplitude, f_1 corresponds to the fundamental frequency, φ is the phase angle, and ξ represents the DC component. In discrete-time, a sequence of N samples with $t = nT_s$, where T_s is the sampling period, the following signal model may be derived

$$s(n)=A\cos(\omega n+\varphi)+\xi^{n/f_s} \tag{15}$$

where $n=0,1,...N$, $f_s=1/T_s$, and $\omega=2\pi f_1/f_s$.

Then, this model is segregated in terms of the sinusoidal component at the fundamental frequency ($s_{ac}(n)$) and a DC component ($s_{dc}(n)$) as:

$$s(n)=s_{ac}(n)+s_{dc}(n) \tag{16}$$

Thus, applying the Z-transform, $s(n)$ can be represented in the Z-domain as [31]

$$\begin{aligned} S(Z) &= S_{ac}(Z)+S_{dc}(Z) \\ &= \frac{A(\cos\varphi-\cos(\omega-\varphi)Z^{-1})}{1-2\cos\omega Z^{-1}+Z^{-2}}+\frac{1}{1-\xi Z^{-1}} \\ &= \frac{B(Z)}{E(Z)} \end{aligned} \tag{17}$$

Whose frequency is computed by the poles in (17), as [31]:

$$E(Z)=Z^0-(C+\xi)Z^{-1}+(1+C\xi)Z^{-2}-\xi Z^{-3} \tag{18}$$

where $C=2\cos\omega$.

Its time discrete representation is achieved by taking the inverse of Z-transform, resulting in [31]

$$E(n)=s_n-U_1 s_{n-1}+U_2 s_{n-2}-U_3 s_{n-3} \tag{19}$$

To find the coefficients in (18), the following linear system is defined from (19):

$$\begin{bmatrix} s_n \\ s_{n-1} \\ s_{n-2} \end{bmatrix} = \begin{bmatrix} U_1 s_{n-1}-U_2 s_{n-2}+U_3 s_{n-3} \\ U_1 s_{n-2}-U_2 s_{n-3}+U_3 s_{n-4} \\ U_1 s_{n-3}-U_2 s_{n-4}+U_3 s_{n-5} \end{bmatrix} \tag{20}$$

where

$$\begin{aligned} U_1 &= C+\xi \\ U_2 &= 1+C\xi \\ U_3 &= \xi \end{aligned} \tag{21}$$

The frequency of the signal is gained using (19) and (21) by [31]

$$f=f_s\cos^{-1}(C/2)/(2\pi) \tag{22}$$

Once the frequency is calculated, the signal model parameters (DC component, amplitude, and phase angle) can be estimated.

1) Parameters' estimation: the model in (15) can be re-written in terms of complex exponential functions as

$$s(n)=\Gamma e^{j\omega n}+\Gamma^* e^{-j\omega n}+DC \tag{23}$$

where $\Gamma=\frac{A}{2}e^{j\varphi}$. Then, (23) is shaped in matrix form as [31]

$$\begin{bmatrix} s(0) \\ s(1) \\ \vdots \\ s(N-1) \end{bmatrix} = \begin{bmatrix} 1 & 1 & 1 \\ e^{j\omega(1)} & e^{-j\omega(1)} & 1 \\ \vdots & \vdots & \vdots \\ e^{j\omega(N-1)} & e^{-j\omega(N-1)} & 1 \end{bmatrix} \begin{bmatrix} \Gamma \\ \Gamma^* \\ DC \end{bmatrix} \tag{24}$$

The DC offset component can be computed through the filtering algorithm consisting of A least square solution. Also, the amplitude and phase angle are given by [31]

$$A=2|\Gamma| \tag{25}$$

$$\varphi=\tan^{-1}\left(\frac{Re\{\Gamma\}}{Im\{\Gamma\}}\right) \tag{26}$$

where $Re(\cdot)$ and $Im(\cdot)$ are the real and imaginary parts of the complex Γ, respectively.

The proposed method for the DC component estimation is outlined in Fig. 1. Furthermore, according to [31], the window length depends of the number of components and is given by

$$N=4c+2 \tag{27}$$

where c corresponds to the number of components (DC offset or harmonics), and N is the number of samples of the window length. To estimate the DC component, just one component is needed in (27), then a window length of $N=6$ samples is required.

C. Computational complexity and computational cost

The ER-based phasor estimation computational burden is widely discussed in [30]. For DC offset removal purposes, the computational complexity also encloses the Moore-Penrose pseudoinverse's, SVD's, eigenvalues' and residues' computation resulting in the following complexity $4p^2q+8pq^2+9q^3$ + n^3 + N^2 [30], [33]–[35], where p and q stand for dimensions of matrix $\mathbf{H}$. In contrast, the Z-domain method mainly involves expressions (20)-(24), resulting in the following computational complexity r^3 (20) + $\mathcal{O}(mn^2+(m)n^3)$ (21) + N^2 (24), with m steps. In total, assuming $p=15$, $q=16$, $n=3$ and $N=32$ for the ER-based estimation and $r=3$, $m=10$, $n=3$ and $N=6$ for the ZDM approach, the computational cost defined in terms of the floating-point operations per second (FLOPS) becomes 83035 and 423 for ER and ZDM, respectively. For instance, if the ER-based approach is implemented on a PowerPC 970 MP RISC microprocessor whose processing frequency is up to 1.2GHz and 0.83 ns of instruction cycle time, then the computation time becomes 68.92 μs [36]–[38], which can be executed at least 3 times within a sample time of 260.42 μs, corresponding to a

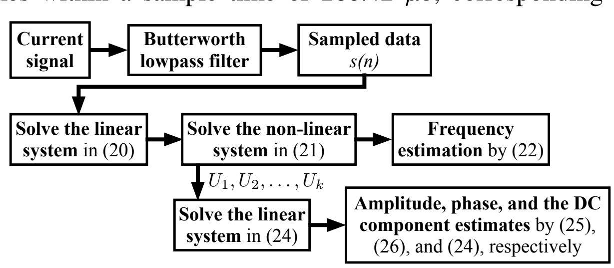

Fig. 1. Flowchart for the Z-domain method.

sampling rate of 64 samples at 60 Hz. The aforementioned analysis makes feasible the phasor estimation implementation in digital processors.

III. Tested Cases

Two study cases for radial and interconnected power grids are enclosed throughout this section. Both cases are detailed describing the fault scenarios considered to acquire the simulated signals that feed the proposed methods in Section II. In this work, signals are acquired by simulation of tested systems in Figs. 2 and 3. A second order low-pass filter type Butterworth (360 Hz cutoff frequency) is employed as anti-aliasing filter for both current and voltage channels. Signals are measured in the *abc* reference frame and transformed into symmetrical components *positive, negative, and zero* prior to estimating the transmission line impedance.

A. Test systems

The applicability and perfomance of the proposals have been tested over two power systems: (*i*) a radial test power system, see Fig. 2; and (*ii*) the IEEE New England 39-bus power grid modeled in DIgSILENT©PowerFactory that is composed by 10 synchronous generators, 39 buses, 12 transformers, 34 transmission lines, and 19 power system loads, as it is shown in Fig. 3. This test system has been extensively used in the power system dynamics literature because exhibit the dynamic properties of a large system [39]. Generators G2 to G10 belong to the New England system and G1 is an equivalent generator that represents the interconnection with the New York power grid. The former is simulated on a commercial software PSCAD© environment to carry out electromagnetic transient simulations including different fault conditions with the features shown in Table I. The latter is implemented in DIgSILENT©PowerFactory executing the study cases summarized in Table II. The simulations are executed using a sampling rate of 1920 Hz, equivalent to 32 samples per cycle.

To evaluate the capability of removing the DC offset by the proposed algorithms and estimating the line impedance in distance relays, three cases are employed with the following disturbances:

- Case 1. Single-phase fault in radial test system: a permanent single-phase fault in phase a at the end of line 1 with a fault resistance $R_F = 10\Omega$.

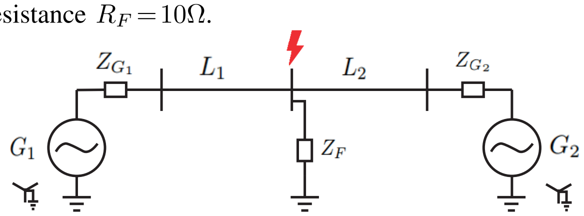

Fig. 2. Simulated power system in PSCAD© for offline training and validation.

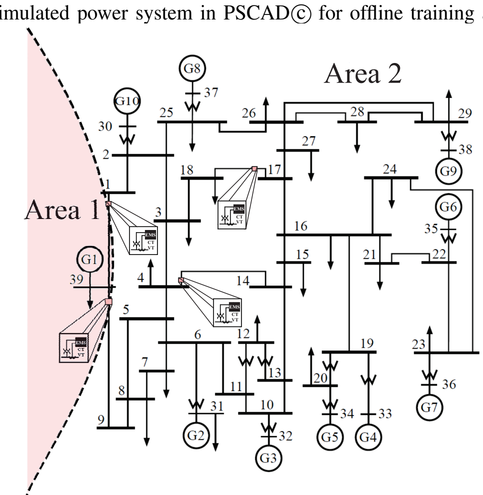

Fig. 3. New England power grid with 10-machine and 39-bus.

TABLE I

Power system characteristics in PSCAD©.

	Lines (Case 1)		
	R [Ω]	X[Ω]	Length [km]
L1	1.0137	12.7032	25
L2	0.3574	5.0776	5

TABLE II

Study cases IEEE New England 39-bus system .

Case	From substation	To substation	Phase fault	Length (%)
2	Northfield (01)	Leeds (39)	B	20
3	Millbury (17)	Carpenter Hill (18)	C	50
4	Millbury (17)	Carpenter Hill (18)	ABC	40

- Case 2. Single-phase fault in phase b in mesh power grid: a permanent line-to-ground fault with a fault resistance of 1Ω that takes place at 20% of the line length between Northfield (bus 01) and Leeds (bus 39) buses.
- Case 3. Single-phase fault in phase c in mesh power grid: a permanent line-to-ground fault with a fault resistance of 1Ω that occurs at the middle point of the transmission line between Millbury (bus 17) and Carpenter Hill (bus 18) buses.
- Case 4. Three-phase fault in mesh power grid: a permanent three-phase fault with a fault resistance of 0Ω that takes place at 40% of the transmission line between Millbury (bus 17) and Carpenter Hill (bus 18) substations.

IV. Numerical Results

In this section, the ER-based and ZDM methods are numerically implemented to precisely estimate current and voltage phasors. Which are subsequently embedded into a strategy to estimate the transmission lines impedance aiming to remove the exponential decaying DC component.

A. Steady-state performance assessment

The steady-state performance is assessed via the frequency response of the filter. For the ER-based and ZDM estimators, their frequency responses correspond to a one-cycle rectangular window of their impulse responses, and they are compared with the well-known DFT, whose frequency response is computed from the DFT coefficients using a one-cycle analysis window [30]. Figure 4 showcases the frequency response to a one-cycle analysis window with 64 samples per fundamental cycle when a frequency offset of 12 Hz is applied to illustrate the frequency tracking for the proposed approaches. It is noteworthy that both approaches exhibit a similar performance, displaced their unit gain at the actual fundamental frequency to 72 Hz. In addition, the proposed estimators deal with the infiltration of the negative fundamental component at -72 Hz, where a zero gain for both algorithms is displayed. This stopband suggests a better rejection of the negative fundamental component.

B. Dynamic performance assessment

The dynamic performance is extensively evaluated through the transient response by time-domain simulations and using multiple study cases. Since a permanent single-phase fault is applied, the relay's voltage and current measurements, for example, for a fault in phase a become: $V_{relay} = V_a$ and $I_{relay} = I_a + k_0 I_0$, with $k_0 = (Z_0 - Z_1)/3Z_1$, where Z_1, and Z_0 are the positive and

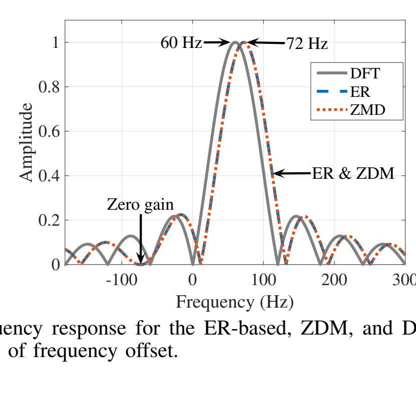

Fig. 4. Frequency response for the ER-based, ZDM, and DFT filters in one cycle for 20% of frequency offset.

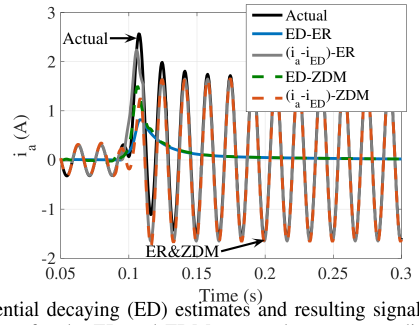

Fig. 5. Exponential decaying (ED) estimates and resulting signals after removing the ED DC offset for the ER and ZDM approaches corresponding to the current signal in phase a for *Case 1*.

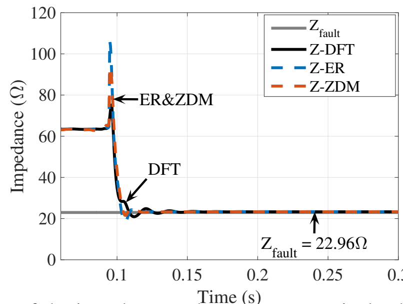

Fig. 6. Behavior of the impedance under a permanent single-phase fault in phase a at the end of line 1 for *Case 1*.

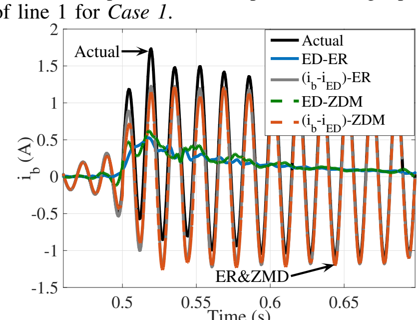

Fig. 7. Exponential decaying estimates and resulting signals without ED for the ER-based and ZDM algorithms corresponding to the current signal in phase b for *Case 2*.

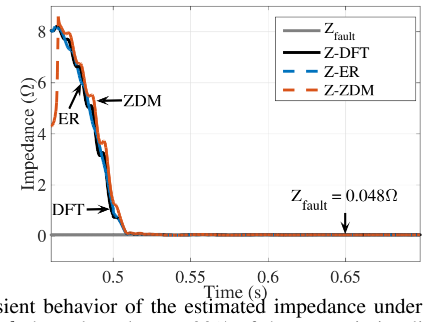

Fig. 8. Transient behavior of the estimated impedance under a line-to-ground fault in phase b that takes place at 20% of the transmission line in *Case 2*.

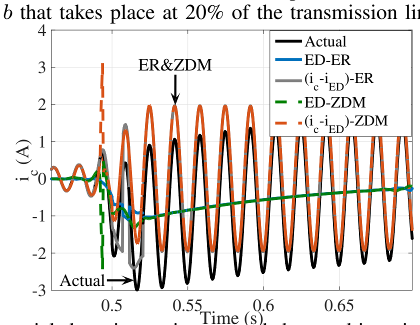

Fig. 9. Exponential decaying estimates and the resulting signals without ED for the ER-based and ZDM algorithms, corresponding to the current signal in phase c for *Case 3*.

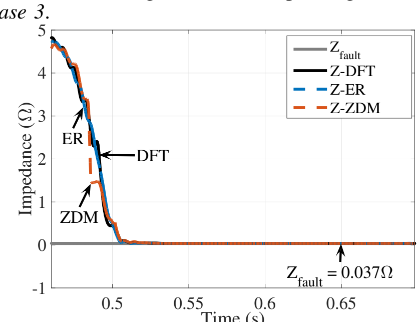

Fig. 10. Transient behavior of the estimated impedance under a line-to-ground fault in phase c at 50 % of the transmission line between Millbury (bus 17) and Carpenter Hill (bus 18) buses, *Case 3*.

zero-sequence impedances, respectively. I_0 is the zero-sequence current. Such measures are employed to estimate the line transmission impedance for these cases, as tackle in the following.

1) Case 1: Figure 5 depicts the exponential decaying (ED) DC offset estimates by the ER-based (ED-ER in blue continuous line) and ZDM filters (ED-ZDM in green dotted line) from the actual signal current (black continuous line). Also, the resulting signals $(i_a - i_{ED})$ after removing the DC offset are respectively shown in gray continuous line for ER and in orange dotted line for ZDM.

On the other hand, the estimated fault impedance reached by the proposed algorithms (ER and ZDM) is compared with the DFT filter. Notice that it converges to the real fault impedance $(Z_{fault} = 22.96\Omega)$, as exhibited in Fig. 6. Besides, it is remarked that both methods prevent the oscillatory behavior in the impedance estimation, disappearing at the same time that the exponential decaying (blue dotted line for ER and orange dotted line for ZDM).

2) Case 2: in this case, the exponential decaying estimates and the resulting signals without ED for the ER-based and ZDM algorithms corresponding to the current signal in phase b are shown in Fig. 7. Similar color notations are used as in *Case 1*. The oscillatory behavior in the current signal is segregated for both methods (ED-ER and ED-ZDM) through the DC offset component removal, resulting in sinusoidal resulting signals $(i_b - i_{ED})$ after one-cycle.

Figure 8 illustrates the impedance estimation by the proposed algorithms and their comparison with the DFT filter. All methods converge to the actual fault impedance value, $Z_{fault} = 0.048\Omega$, which is attained in a similar way.

3) Case 3: Figure 9 displays the ED estimates and the resulting signals after their segregation in the actual signal (a permanent single-phase fault at phase c). Notice that both strategies also prevent the negative DC offset when the fault takes place in the negative semi-cycle, resulting in a smoothed impedance estimation, as depicted in Fig. 10, where the proposed methods and the DFT filter reaches the actual impedance fault value similarly $(Z_{fault} = 0.037\Omega)$.

4) Case 4: Figure 11 illustrates the currents in the abc reference frame when a permanent three-phase fault is applied. The estimated fault impedance reached by the ER-based, ZDM, and DFT techniques converges to the actual impedance fault value $(Z_{fault} = 3.9182\Omega)$, as can be evidenced in Fig. 12. This corresponds to the 40 % of the line impedance between Millbury (bus 17) and Carpenter Hill (bus 18) buses whose value is $Z_1 = 0.83317 + 9.760051i\Omega$.

V. Conclusions

This paper have effectively demonstrated the exponential decaying DC offset removal via the introduction of two novel methods: the ER-based system identification and Z-domain. Both techniques appropriately extract voltage and currents phasor at the fundamental frequency, facilitating the impedance

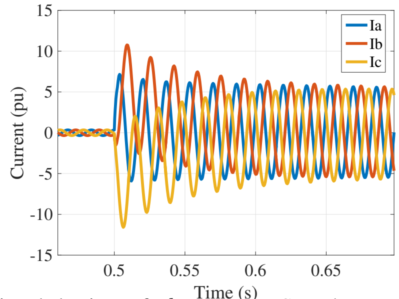

Fig. 11. Transient behaviour of *abc* currents, *Case 4*.

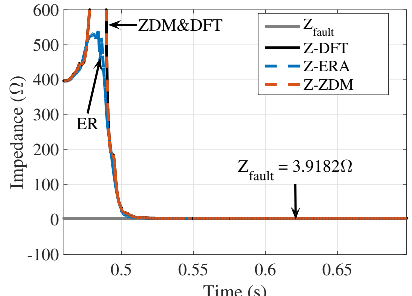

Fig. 12. Transient behavior of the estimated impedance under a three-phase fault at 40 % of the transmission line between Millbury (bus 17) and Carpenter Hill (bus 18) buses, *Case 4*.

estimation process in distance relays under single-phase faults. They last one-cycle for providing phasor estimates used in the transmission line impedance estimation and mitigate the overreach and underreach caused by the oscillatory behavior in the impedance estimation. They also provide better estimates under fault conditions, because it rejects the exponentially decaying DC offset. It is noteworthy the straightforward applicability of the Z-domain method since it only needs 6 samples to estimate the ED component and remove it for the current signal phasor, i.e., less than a fifth of the one-cycle window. Furthermore, after assessing both estimators under steady-state and dynamic conditions, it is possible to guarantee the great potential for applying them to line protection as the distance relay, where it exhibits shorter time or a lower number of samples for reaching the objective.

References

[1] Jyh-Cherng Gu and Sun-Li Yu, "Removal of dc offset in current and voltage signals using a novel fourier filter algorithm," *IEEE Trans. Power Del.*, vol. 15, no. 1, pp. 73–79, 2000.

[2] A. Yusuff, A. Jimoh, and J. Munda, "Stationary wavelet transform and single differentiator based decaying dc-offset filtering in post fault measurements," *Measurement*, vol. 47, pp. 919 – 928, 2014.

[3] Z. Jiang, S. Miao, and P. Liu, "A modified empirical mode decomposition filtering-based adaptive phasor estimation algorithm for removal of exponentially decaying dc offset," *IEEE Trans. Power Del.*, vol. 29, no. 3, pp. 1326–1334, 2014.

[4] M. S. Sachdev and M. A. Baribeau, "A new algorithm for digital impedance relays," *IEEE Trans. Power App. Syst.*, vol. PAS-98, no. 6, pp. 2232–2240, 1979.

[5] E. O., S. III, and D. Hou, "Filtering for protective relays," pp. 1–26, 1995.

[6] E. Rosołowski, J. Iżykowski, and B. Kasztenny, "Adaptive measuring algorithm suppressing a decaying dc component for digital protective relays," *Electr. Power Syst. Res.*, vol. 60, no. 2, pp. 99–105, 2001.

[7] J. Lambert, A. G. Phadke, and D. McNabb, "Accurate voltage phasor measurement in a series-compensated network," *IEEE Trans. Power Del.*, vol. 9, no. 1, pp. 501–509, 1994.

[8] S. Kang, D. Lee, S. Nam, P. A. Crossley, and Y. Kang, "Fourier transform-based modified phasor estimation method immune to the effect of the dc offsets," *IEEE Trans. Power Del.*, vol. 24, no. 3, pp. 1104–1111, 2009.

[9] C. D. L. da Silva, G. C. Junior, A. P. de Morais, G. Marchesan, and F. G. K. Guarda, "A continually online trained impedance estimation algorithm for transmission line distance protection tolerant to system frequency deviation," *Electr. Power Syst. Res.*, vol. 147, pp. 73–80, 2017.

[10] R. C. Dos Santos and E. C. Senger, "Transmission lines distance protection using artificial neural networks," *Int. J. Electr. Power Energy Syst.*, vol. 33, no. 3, pp. 721–730, 2011.

[11] H. Hajizadeh, S.-A. Ahmadi, and M. Sanaye-Pasand, "An analytical fast decaying dc mitigation method for digital relaying applications," *IEEE Trans. Power Del.*, 2020.

[12] A. Phadke and J. Thorp, *Synchronized Phasor Measurements and Their Applications*, ser. Power Electronics and Power Systems. Springer US, 2008. [Online]. Available: https://books.google.com.co/books?id=sCk3mK4kCWwC

[13] G. Benmouyal, "Removal of dc-offset in current waveforms using digital mimic filtering," *IEEE Trans. Power Del.*, vol. 10, no. 2, pp. 621–630, 1995.

[14] E. Vázquez, A. Zamora-Mendez, M. R. A. Paternina, L. A. Trujillo-Guajardo, and A. Jose, "Dynamic phasor-driven digital distance relays protection," *Elect. Power Syst. Res.*, vol. 184, p. 106316, 2020.

[15] A. Zamora, J. M. Ramirez, M. R. A. Paternina, and E. Vazquez-Martinez, "Digital filter for phasor estimation applied to distance relays," *IET Gener. Transm. Distrib.*, vol. 9, no. 14, pp. 1954–1963, 2015.

[16] J. G. Proakis, *Digital signal processing: principles algorithms and applications*. Pearson Education India, 2001.

[17] A. G. Phadke and J. S. Thorp, *Computer relaying for power systems*. John Wiley & Sons, 2009.

[18] A. Rahmati and R. Adhami, "An accurate filtering technique to mitigate transient decaying dc offset," *IEEE Trans. Power Del.*, vol. 29, no. 2, pp. 966–968, 2014.

[19] M. Pazoki, "A new dc-offset removal method for distance-relaying application using intrinsic time-scale decomposition," *IEEE Trans. Power Del.*, vol. 33, no. 2, pp. 971–980, 2018.

[20] K. W. Min and S. Santoso, "Dc offset removal algorithm for improving location estimates of momentary faults," *IEEE Trans. Smart Grid*, vol. 9, no. 6, pp. 5503–5511, 2018.

[21] A. A. Abdoos, S. A. Gholamian, and M. Farzinfar, "Accurate and fast dc offset removal method for digital relaying schemes," *IET Gener. Transm. Distrib.*, vol. 10, no. 8, pp. 1769–1777, 2016.

[22] F. F. Costa, D. A. Formiga, R. R. Ferreira, T. Sousa, and F. B. Costa, "A recursive least-squares aided by pre-filtering for phasor-estimation in distance protection," in *IEEE Grenoble Conf.*, 2013, pp. 1–6.

[23] H. Jiali, D. Yuqian, L. Yongli, W. Gang, and L. Shanshan, "Distance relay protection based on artificial neural network," 1997.

[24] Y. Li, B. Li, X. Zhang, and J. He, "An ann-based distance protective relays of transmission lines," 2001.

[25] M. Tawfik and M. Morcos, "Ann-based techniques for estimating fault location on transmission lines using prony method," *IEEE Trans. Power Del.*, vol. 16, no. 2, pp. 219–224, 2001.

[26] J. Bay, *Fundamentals of Linear State Space Systems*, ser. Electrical Engineering Series. WCB/McGraw-Hill, 1999.

[27] J.-N. Juang and R. S. Pappa, "An eigensystem realization algorithm for modal parameter identification and model reduction," *J. Guid Control Dyn*, vol. 8, no. 5, pp. 620–627, 1985.

[28] R. A. D. Callafon, B. Moaveni, J. P. Conte, X. He, and E. Udd, "General realization algorithm for modal identification of linear dynamic systems," *J. Eng. Mechan.*, vol. 134, no. 9, pp. 712–722, 2008.

[29] V. Klema and A. Laub, "The singular value decomposition: Its computation and some applications," *IEEE Trans. Autom. Control*, vol. 25, no. 2, pp. 164–176, 1980.

[30] A. Zamora-Mendez, F. Zelaya-A., J. A. de la O Serna, J. H. Chow, and M. R. Arrieta Paternina, "Model-based synchrophasor estimation by exploiting the eigensystem realization approach," *Electr. Power Syst. Res.*, vol. 182, p. 106249, 2020.

[31] S.-C. Julián, G.-R. J. Alberto, J. Brian, M. Pablo, and G. Armando, "Time domain parameter identification of transient electromechanical oscillations," *COMPEL - The Int. J. for Compu. and Mathem. in Elect. and Electronic Eng.*, vol. 38, pp. 574–595, 2019.

[32] J. Sotelo Castañon, "Development of a new method for the characterization of multicomponent sinusoidal signals with time-varying parameters," Ph.D. dissertation, CINVESTAV, Guadalajara,Mexico, 6 2016.

[33] M. C. Seiler and F. A. Seiler, "Numerical recipes in c: the art of scientific computing," *Risk Analysis*, vol. 9, no. 3, pp. 415–416, 1989.

[34] Campar. 3d computer vision script. singular value decomposition. [Online]. Available: https://es.scribd.com/document/203682182/3DCV-svd-000, urldate = 2018-07-18

[35] T. H. Cormen, C. E. Leiserson, R. L. Rivest, and C. Stein, *Introduction to algorithms*. MIT press, 2009.

[36] *TI (2012, Aug). TMS320F28335 Digital Signal Controllers. Data Manual.*, Texas Instruments Inc., Dallas, Texas. [Online]. Available: http://www.ti.com/lit/ds/sprs439m/sprs439m.pdf.

[37] *TI (1991, Aug). TMS320 Second-Generation Digital Signal Processors. Data Manual.*, Texas Instruments Inc., Dallas, Texas. [Online]. Available: http://pdf.datasheetcatalog.net/datasheets/700/315970_DS.pdf.

[38] *IBM (2008, Jan). PowerPC 970MP RISC Microprocessor. Version 1.3.*, International Business Machines Corp.,, Hopewell Junction, NY.

[39] "Phase ii: frequency domain analysis of low-frequency oscillations in large electric power systems. volume 1: Basic concepts, mathematical models and computing methods," *Elect. Power Res. Inst.*, April 1982.